Load Sharing and Profile Modification of Spur Gear Teeth in the General Case of any Flank Geometry

G. K. Nikas, London/UK

1. INTRODUCTION

It had been quite early recognised that the life of spur gears with straight teeth, as well as noise and vibrations, can be significantly "improved" by the application of an appropriate tooth profile modification in order to minimize the dynamic effects which result from abrupt changes of the static load distribution during a mesh cycle ([1]). This is especially obvious for low-contact-ratio spur gears. In reference [2] for example, it was shown that noise can be reduced by up to 10 dBA after a tooth profile optimization. In reference [3] it is clearly shown how a tooth profile modification can increase the scoring resistance of spur gears. A dramatic effect of tooth dynamic loading is demonstrated in [4] and [5] where it is shown that the variable tooth stiffness and flank errors may sometimes cause separation of two teeth during cooperation which further results in severe stresses and even in tooth breakage!

To avoid all these destructive effects of tooth variable stiffness and profile errors, one may reduce the power-to-weight-ratio. A much better and preferable solution is to do an appropriate tooth flank modification. For this reason tooth compliance and tooth errors (operational, undercuts, pits etc.) have to be accurately known.

In a previous work ([6]) the author presented a complete and accurate method for the calculation of the optimum profile modification, a method which has experimental verification (for example, there is only a 3 percent deviation between the results of reference [6] and the experimental results of reference [3]). That method omitted tooth errors. In the present work, the method has been extended to cover the general case of profile errors of any form and therefore it is referred to as a general flank geometry method. Also the case of flank geometries other than the standard involute can rather easily be adapted by using the Generalized Theory of Gearing ([6], [7]). The advantages of the present method are: generality, accuracy and speed. Compared with FEM methods for the calculation of tooth stiffness, increase of speed is more than significant since the computer program written for the present work needs only 1 sec of CPU time of a PC with a Pentium processor to complete all calculations, using 1000 nodes for the discritization of a tooth flanks!

Although the case of internal involute spur gears was initially intented to be covered here, it was decided that it deserves a separate publication. This paper serves as a robust tool to spur gear designer and as a detailed guide to gear manufacturer for the purpose of creating low-noise and long-life gears for today's demanding applications.

2. TOOTH COMPLIANCE

Teeth deflect elastically as a result of the applied load. As a consequense of this deflection, the load distribution between one and two (or more) pair of teeth during a mesh cycle changes compared to that in the case of ideal rigid teeth. Premature engagement and delayed disengagement take place and teeth suffer from excesive stresses at the tip and fillet area. The tip area may sometimes undergo plastic deformations and significant flash temperatures that cause scuffing failure.

The ammount of tooth deflection can be calculated according to the equations of Weber [8], Attia [9] and Cornell [10]. These equations comply well with finite element results and can be safely used as a good approximation of the real thing. More specifically, three kinds of deflection are considered:

(1) Bending deflection which is the displacement of the tooth axis of symmetry with the root of the tooth being unflexible. It incorporates bending moments and shear and normal forces.

(2) Deflection due to local surface Hertzian compression.

(3) Deflection of the tooth's root due to the flexibility of the tooth's base (assuming that the rest of tooth's body remains rigid).

We define now a compliance coefficient C that will be used throughout this text:

$$C = \frac{\delta \cdot E \cdot b}{W} \tag{1}$$

where

δ : normal tooth deflection along the line of action

E : modulus of elasticity

b : face width of the gear

W : normal tooth load along the line of action

The total deflection of a pair of cooperating teeth is the sum of all individual deflections of each tooth. So:

$$\delta = \delta_{B,1} + \delta_{F,1} + \delta_{B,2} + \delta_{F,2} + \delta_{H} \tag{2}$$

where subsripts 1 and 2 refer to pinion and gear respectively. Subscripts B, F and H refer to bending, foundation and Hertz compliance respectively. Using Eq. (1) and defining the effective Young's modulus of a teeth pair as

$$E = 2 \cdot \frac{E_1 \cdot E_2}{E_1 + E_2} \tag{3}$$

the total compliance coefficient for the teeth pair is:

$$C = C_H + \frac{2}{E_1 + E_2} \cdot \left[E_1 \cdot (C_{B,2} + C_{F,2}) + E_2 \cdot (C_{B,1} + C_{F,1}) \right] \tag{4}$$

2.1 BENDING COMPLIANCE

Bending deflection is calculated assuming that the tooth is an elastic beam based on a rigid foundation (see Fig. 1). Equating the external work done by load W to the work of internal forces N, Q and moment M, we get:

$$W \cdot \delta = \int_0^Y \left[\frac{M^2}{E \cdot I} + K \cdot \frac{Q^2}{G \cdot A} + \frac{N^2}{E \cdot A} \right] dy \tag{5}$$

where

M : bending moment, $M = (y - Y) \cdot Q$ (Fig. 1)

I : moment of inertia, $I = b \cdot t^3 / 12$ where t is tooth's thickness at position y (Fig. 1)

K : shape form factor of tooth cross sectional area. For rectangular areas, the theory of elasticity gives that $K = (12 + 11 \cdot \nu)/(10 + 10 \cdot \nu)$ where ν is the Poisson ratio.

Q : shear load component, $Q = W \cdot \cos(\phi)$ (Fig. 1)

G : shear modulus, $G = E/(2 + 2 \cdot \nu)$

A : tooth cross sectional area, $A = b \cdot t$

N : radial load component, $N = W \cdot \sin(\phi)$ (Fig. 1)

Using Eqs (1) and (5), the bending compliance coefficient is

$$C_B = \cos^2(\phi) \cdot \left\{ 12 \cdot I_2 + [2.4 + 2.2 \cdot \nu + \tan^2(\phi)] \cdot I_1 \right\} \tag{6}$$

where

$$I_1 \equiv \int_0^Y \frac{1}{t} dy \qquad \text{and} \qquad I_2 \equiv \int_0^Y \frac{(y - Y)^2}{t^3} dy \tag{7}$$

Integrals I_1 and I_2 are calculated numerically using the extended trapezoid rule since the integration step is not constant. The calculation of angle ϕ, distance Y and thickness t is done here in the general case of any flank geometry. For this reason, the Generalized Theory of Gearing (GTG) ([6], [7]) is used. The equations of that theory will not be repeated here. Using Fig. 1, angle ϕ is the angle between the line of load action and line AB. Through the GTG, the position of the whole tooth body is known at every instant during a mesh cycle. Therefore, points A and B are also known. Angle ϕ is:

$$\phi = \arctan \left[\frac{x_B \cdot (y_B - y_A) - y_B \cdot (x_B - x_A)}{x_B \cdot (x_B - x_A) + y_B \cdot (y_B - y_A)} \right] \tag{8}$$

Y is the distance of point C (Fig. 1) and line AB (which is known as already said):

$$Y = d\left\{[(\text{line of load action}) \cap (\text{tooth's centre-line})], AB\right\}$$

Point C belongs to the line of load action and to the tooth's centre-line, which are known through the GTG. Therefore distance Y can easily be found. Finally, thickness t can be calculated straightforwardly because tooth's flanks are exactly known from the GTG for any geometry.

2.2 HERTZ COMPLIANCE

Following Weber's analysis [8], it is assumed that the compression effect of tooth's load extends from contact point E down to the tooth's centre-line (Fig. 2). The Hertz compliance coefficient is given by the following equation:

$$C_H = \frac{2\cdot(1-\nu^2)}{\pi}\cdot\left[\ln\left(\frac{4\cdot h_1\cdot h_2}{c^2}\right) - \frac{\nu}{1-\nu}\right] \quad (9)$$

where

$$c^2 = \frac{8\cdot W\cdot \rho_1\cdot\rho_2\cdot(E_1+E_2)\cdot(1-\nu^2)}{\pi\cdot b\cdot E_1\cdot E_2\cdot(\rho_1+\rho_2)} \quad (10)$$

$$\nu^2 = 1 - \frac{E_1\cdot E_2}{E_1+E_2}\cdot\left(\frac{1-\nu_1^2}{E_1} + \frac{1-\nu_2^2}{E_2}\right) \quad (11)$$

whereas E_1, E_2, ν_1, ν_2 are moduli of elasticity and Poisson ratios for each one of the cooperating teeth respectively. Distances h_1 and h_2 are easily calculated according to what is written in paragraph 2.1. The radii of curvature ρ_1 and ρ_2 can be found for any tooth flank geometry according to a previous work of the author ([11]), but the lengthy analysis of [11] will not be repeated here. It must be mentioned that since the Hertz compliance coefficient C_H is a function of load W which depends on tooth's compliance on its turn, a prediction-correction loop is necessary to assure small errors in the calculations. Using an under-relaxation factor of 0.3, these errors are minimized to practically zero fast.

2.3 FOUNDATION COMPLIANCE

Following Attia's [9] analysis, verified by Cornell [10], the foundation compliance coefficient C_F is:

$$C_F = (1 - \nu^2)\cdot\cos^2(\phi)\cdot\left\{\frac{50}{3\cdot\pi}\cdot\left(\frac{Y}{t_F}\right)^2 + \frac{2 - 4\cdot\nu}{1 - \nu}\cdot\frac{Y}{t_F} + \frac{4.82}{\pi}\cdot\left[1 + \right.\right.$$

$$\left.\left. + \frac{\tan^2(\phi)}{2.4\cdot(1 + \nu)}\right]\right\} \qquad (12)$$

Variables ϕ and Y are calculated according to paragraph 2.1. Constant t_F (Fig. 1) can easily be found since points A and B are knonw in space through the GTG, as was explained in paragraph 2.1.

3. STATIC LOAD DISTRIBUTION

The analysis of this paragraph is limited to spur gears with contact ratios less than 2, where the dynamic phenomena are more intense. Fig. 3 shows a typical load sharing curve for rigid gears. Teeth engage at point A and disengage at B. Along A'B' the load is transmitted through only one pair of teeth whereas along AA' and B'B there are two pairs of teeth in cooperation. To avoid interference or loss of contact when two pairs of teeth are in cooperation, transmission errors at the points of contact have to be equal. Therefore, along the line of load action:

$$\delta_1 + e_1 + \lambda_1 = \delta_2 + e_2 + \lambda_2 \qquad (13)$$

where

δ : deflection due to compliance of a teeth pair,

e : relative manufacturing and/or operational errors,

λ : flank profile modifications.

Subscripts 1 and 2 refer to the first and second pair of teeth in contact respectively. Each pair of teeth in contact bears its own part of total load such as:

$$W_1 + W_2 = W \qquad (14)$$

Using Eqs (13), (14) and (1), individual loads W_1 and W_2 can be found as follows:

$$W_1 = \frac{W\cdot C_2 + E\cdot b\cdot(e_2 + \lambda_2 - e_1 - \lambda_1)}{C_1 + C_2} \qquad (15)$$

$$W_2 = \frac{W \cdot C_1 - E \cdot b \cdot (e_2 + \lambda_2 - e_1 - \lambda_1)}{C_1 + C_2} \tag{16}$$

In case of one pair of teeth in contact, $W_1 = W$.

4. FLANK PROFILE MODIFICATION

In order to obtain a smooth static load sharing without the abrupt changes shown in Fig. 3, profile modification is applied at the tips (only) of the teeth of both pinion and gear. According to [12] this tactic is superior to the ones where only pinion or only gear teeth flanks are modified. The incorporation of flank error functions in the equations is necessary because there are cases where flank errors cover part of profile modifications in the ideal case of teeth flanks without errors and in other cases the opposite is true. If κ is the necessary profile modification when teeth flank errors are neglected (as it is calculated for example in [6]), then:

if $e > \kappa$ then gears can not be optimized or repaired

if $e \leq \kappa$ then gears can be repaired and optimized

Obviously, only cases where $e \leq \kappa$ will be treated in this paper. Two different methods are used.

4.1 PROFILE MODIFICATION BASED ON CONTACT PATH MODIFICATION

This method is appropriate when teeth pair errors are a smooth, monotonous function of position along the end parts of the path of contact. In other words it can be used when the errors are of the same form as the modification of contact path shown in Fig. 4. Following the notation of Fig. 4 (which refers to involute geometry for simplicity), the proposed modification of the path of contact abcd is:

$$\lambda = \lambda_a \cdot \left(1 - \frac{x}{x_b}\right)^z \qquad 0 \leq x < x_b \tag{17}$$

$$\lambda = 0 \qquad x_b \leq x < \epsilon - x_c \tag{18}$$

$$\lambda = \lambda_d \cdot \left(1 - \frac{\epsilon - x}{x_c}\right)^z \qquad \epsilon - x_c \leq x \leq \epsilon \tag{19}$$

where ϵ is the contact ratio and exponent z can be chosen in a way to obtain the smoothest load distribution, as will be shown later. If the load at points a and d of Fig. 4 is taken to be zero and assuming that $e_b = e_c = 0$ (no errors at points b and c) then from Eqs (15) and (16) we get:

$$\lambda_{a,profile} = \frac{W \cdot C_c}{E \cdot b} - e_a \quad \text{and} \quad \lambda_{d,profile} = \frac{W \cdot C_b}{E \cdot b} - e_d \tag{20}$$

λ_a and λ_d of Eqs (17) and (19) refer to the path of contact. The relation between λ and $\lambda_{profile}$ has been found geometrically by the author ([12]) but the analysis is omitted here because it is rather lengthy.

4.2 PROFILE MODIFICATION IN THE GENERAL CASE OF A NON-SMOOTH ERROR FUNCTION

When errors e are not a smooth function of position along the end parts of the contact path, the analysis of the previous paragraph is inappropriate. In such a case either Eq. (15) or (16) is rearranged to give:

$$\lambda_2 - \lambda_1 = \frac{W_1 \cdot (C_1 + C_2) - W \cdot C_2}{E \cdot b} + e_1 - e_2 \tag{21}$$

By choosing the load distribution to be without abrupt changes (e.g. of a trapezoidal form) and consequently by knowing loads W_1 and W_2 along the path of contact the difference of profile modifications λ_1 and λ_2 can be found from Eq. (21). One more equation is necessary in order to calculate λ_1 and λ_2. We can appropriately choose λ_1 (or λ_2) and then calculate λ_2 (or λ_1) from Eq. (21). This choise may be based on the possibility of achieving the intented profile modifications in practice. This method is quite general since it covers effectively the real case of an arbitrary error function along tooth flanks.

5. EXAMPLE AND CONCLUSION

An example with practical interest is quoted here. It refers to involute gears with smooth flank error functions. More specifically, errors of the form

$$e_i = c_i \cdot \lambda_i \quad , \ i = 1,2 \tag{22}$$

where λ is the profile modification in the case of teeth without errors and c is a constant are considered. Constants c_i are as follows:

$$c_1 = -0.2 \quad \text{and} \quad c_2 = 0.6 \tag{23}$$

To show the generality of the method and the accompanying computer program, data for gear teeth have been chosen such as to deviate from known standards. These data are: pressure angle $\alpha_0 = 18^\circ$, module m = 7 mm, rack dedendum $h_f = 1.27 \cdot m$, rack addendum $h_k = 1.1 \cdot m$, number of teeth of pinion $Z_1 = 24$, number of teeth of gear $Z_2 = 33$, teeth width b = 10 mm, transmitted power 80 KW at 10000 RPM. The contact ratio is $\epsilon \approx 1.87$. Fig. 5 shows all compliance coefficients (subscripts "p" and "g" are for pinion and gear respectively). Apart from the Hertz compliance coefficient C_H, all other coefficients are practically the same with those in case of ideal teeth (without flank errors). The Hertz coefficient C_H exhibits a peculiarity because it is load-dependent. This is clearly shown in Fig. 6. The static load curves are shown in Fig. 7. The effect of flank errors on the load distribution is more than obvious. Following the analysis of paragraph 4.1, the smoothest load distribution (for teeth with errors) is found for z = 2 (see Eqs (17) and (19)). If z = 1, the results are not singificantly different. If z > 2, the load curve approaches the one for unmodified teeth, as it was proved in [6]. Finally, Fig. 8 shows the necessary flank modifications to achieve the smooth load distribution of Fig 7, along the path of contact (X_{poc} is the distance from the pitch point). Thus, gear manufacturer knows exactly the amount of flank modification to be done at every point along teeth flanks.

It is therefore shown that the elimination of static load abrupt changes is a target that can be theoretically achieved. All it remains to be done is to evaluate the theoretical results with a series of experiments that will also test the possibility of achieving the proposed flank modifications in practice.

REFERENCES

[1] H. Walker: "Gear tooth deflection and profile modification", The Engineer, October 14, 1938, p. 409

[2] D.W. Barnett and A.K. Sattee: "G-NOISE An analytical approach to

gear profile optimization for low noise emission", 1980 B.G.A. Annual Conference

[3] M. Yokoyama, J. Ishikawa and K. Hayashi: "Effect of tooth profile modification on the scoring resistance of heavy-duty spur gears", Wear, vol. 19, 1972, p. 131

[4] K.L. Wang and H.S. Cheng: "A numerical solution to the dynamic load, film thickness, and surface temperatures in spur gears, Part II Results, ASME trans. (J. of Mechanical Design), vol 103, 1981, p. 188

[5] R. Kasuba and J.W. Evans: "An extended model for determining dynamic loads in spur gearing", ASME trans. (J. of Mechanical Design), vol. 103, 1981, p. 398

[6] Th. Costopoulos and G.K. Nikas: "Minimization of spur gear dynamic loading through the Generalized Theory of Gearing", proceedings of the International Congress - Gear Transmissions '95, 26-28 September 1995, Sofia, Bulgaria, vol. 1, p. 52

[7] Th. Costopoulos: "Generalized theory of gearing and tooth stress", proceedings of the Ninth World Congress on the Theory of Machines and Mechanisms, Politecnico di Milano, Italy, August 29 - September 2 1995, vol. 1, p. 369

[8] C. Weber: "The deformations of loaded gears and the effect on their load-carrying capacity", sponsored research (Germany), British Dept. of Scientific and Industrial Research, Report No. 3, 1949

[9] A.Y. Attia: "Deflection of spur gear teeth cut in thin rims", ASME trans. (J. of Engineering for Industry), 1964, p. 333

[10] R.W. Cornell: "Compliance and stress sensitivity of spur gear teeth", ASME trans. (J. of Mechanical Design), vol. 103, 1981, p. 447

[11] G.K. Nikas and Th. Costopoulos: "Generalized Theory of Gearing and elastohydrodynamic lubrication of spur gears", proceedings of the International Congress - Gear Transmissions '95, 26-28 September 1995, Sofia, Bulgaria, vol. 1, p. 118

[12] G.K. Nikas: "Elastohydrodynamic lubrication and minimization of the dynamic loading of spur gear straight teeth", diploma thesis (in Greek), 1994, National Technical University of Athens, Mechanical Engineering Department, Machine Elements section

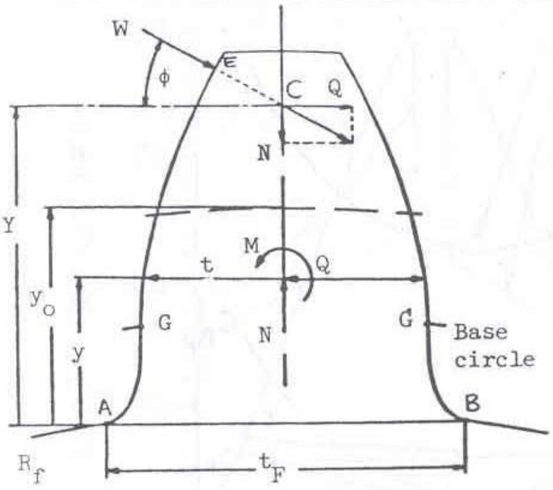

Fig. 1

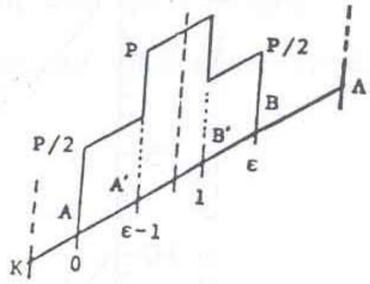

Fig. 3

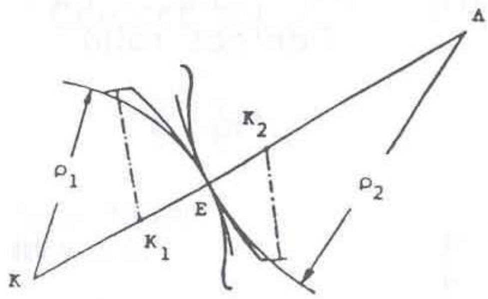

Fig. 2

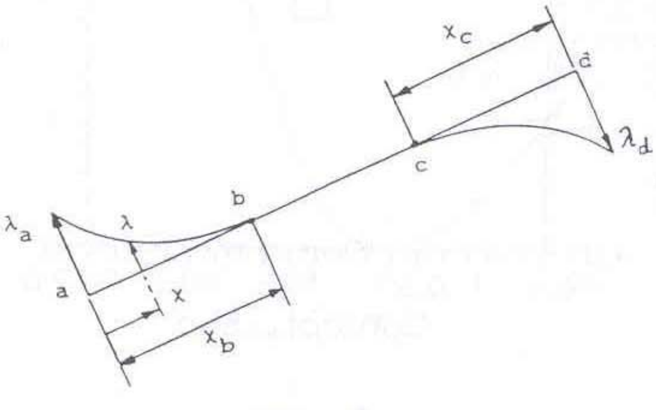

Fig. 4

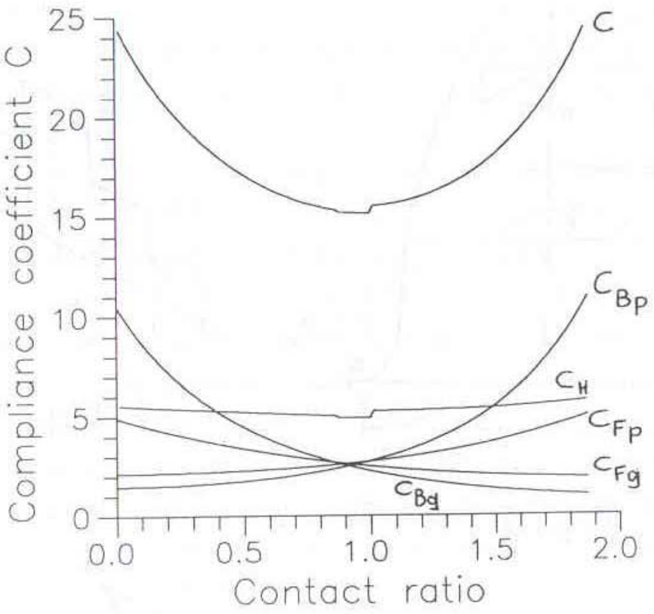

Compliance coefficient C
25
20
15
10
5
0
0.0
0.5
1.0
1.5
2.0
Contact ratio
C
C_{Bp}
C_H
C_{Fp}
C_{Fg}
C_{Bg}

Fig. 5

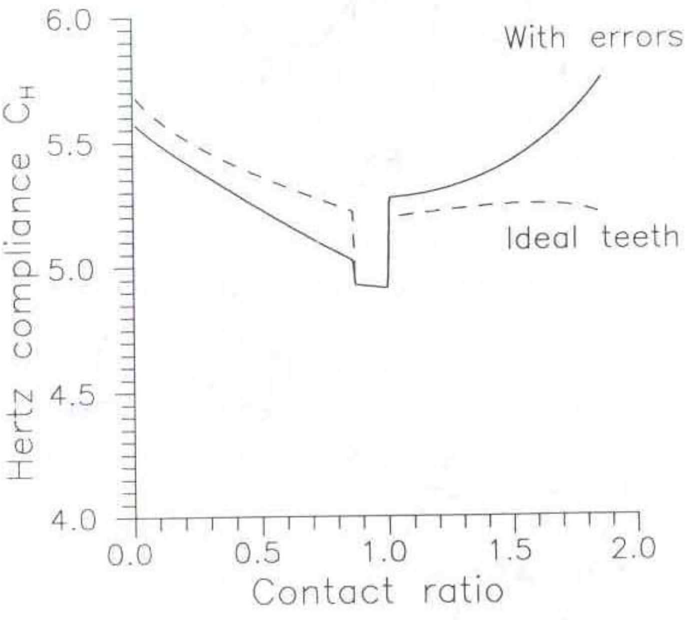

Hertz compliance C_H
6.0
5.5
5.0
4.5
4.0
0.0
0.5
1.0
1.5
2.0
Contact ratio
With errors
Ideal teeth

Fig. 6

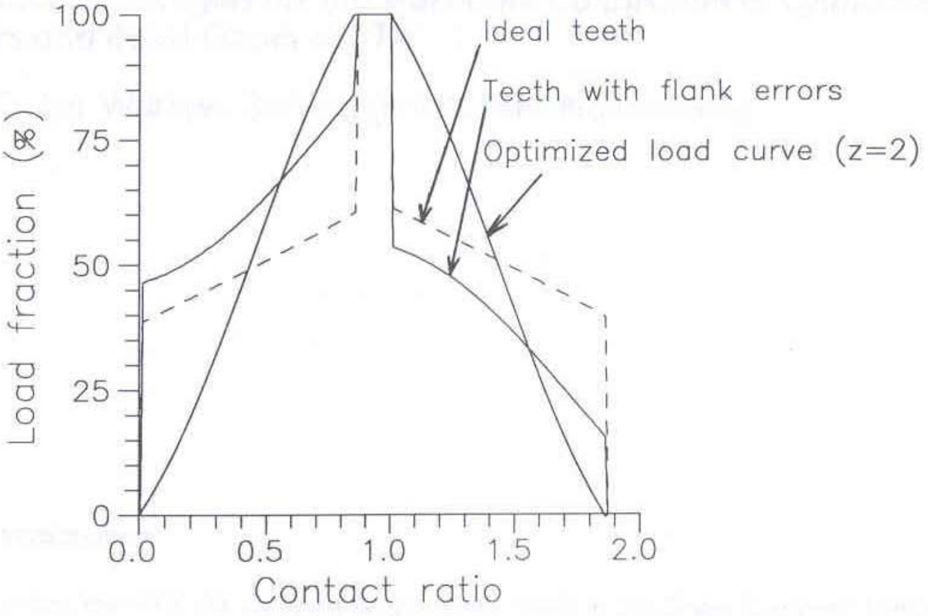
Ideal teeth
Teeth with flank errors
Optimized load curve (z=2)
Load fraction (%)
100
75
50
25
0
0.0
0.5
1.0
1.5
2.0
Contact ratio

Fig. 7

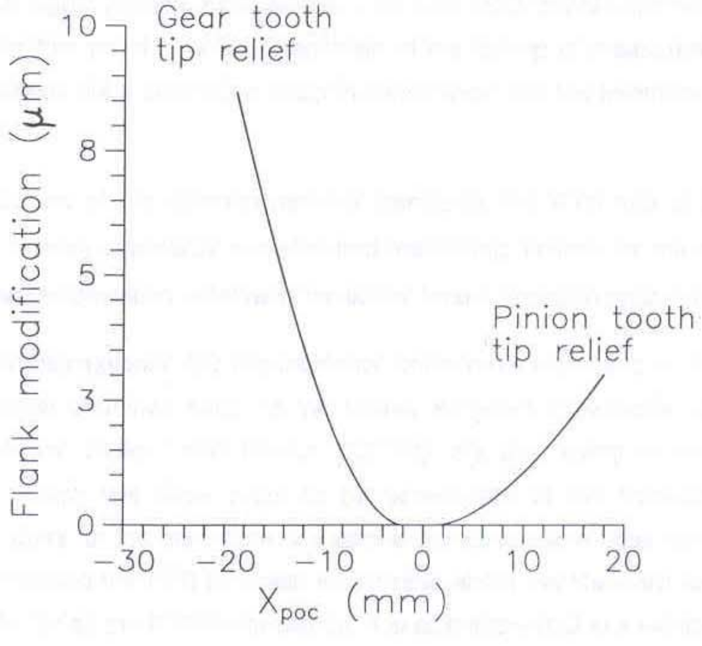
Gear tooth
tip relief
Pinion tooth
tip relief
Flank modification (μm)
10
8
5
3
0
−30
−20
−10
0
10
20
X_{poc} (mm)

Fig. 8